Chemical Physics 23 (1977) 39–50

THEORETICAL STUDIES OF CH_3, CH_3^+ AND CH_3^- USING CORRELATED WAVEFUNCTIONS*

G.T. SURRATT** and W.A. GODDARD III

Arthur Amos Noyes Laboratory of Chemical Physics,‡ California Institute of Technology, Pasadena, California 91125, USA

Received 11 November 1976

Studies of CH_3, CH_3^+ and CH_3^- have been performed using Hartree–Fock, generalized valence bond and configuration interaction wavefunctions, employing a good quality gaussian basis set. The primary emphasis was placed on the calculation of the out-of-plane vibration in CH_3 and CH_3^+ and on the calculation of the electron affinity of CH_3. We find that CH_3 and CH_3^+ are planar with frequencies of $\nu_2 = 585$ cm^{-1} for CH_3 and $\nu_2 = 1570$ cm^{-1} for CH_3^+. This allows us to select between the sets of ν_2 obtained by Herzberg leading to $\nu_2 = 607$ cm^{-1} for CH_3 and $\nu_2 = 1360$ cm^{-1} for the (Rydberg) excited state of CH_3. We find that the outer electron of CH_3^- is not bound.

1. Introduction

General ideas about bonding suggest that CH_3^+, CH_3, and CH_3^- have equivalent hydrogens (a three-fold axis), that CH_3^+ is planar and that CH_3^- is bent (approximately tetrahedral). On the other hand, the planarity of CH_3 is not so obvious from simple bonding ideas, but most evidence points to a planar structure with a small force constant for the umbrella (ν_2) vibration. (See section 5 for further discussion.)

We became interested in these systems for several reasons:

(1) Recent photoelectron spectra of CH_3 were interpreted by Koenig et al. [1] as indicating CH_3 to have a slightly nonplanar geometry.

(2) It appeared to us that CH_3^- might not be bound (that is, that the electron affinity of CH_3 is negative). This was relevant to studies we were carrying out on the surface of diamond and in particular the electron affinity of the diamond surface.

(3) There was some confusion in the literature with regard to the vibrational frequencies for the ν_2 mode in CH_3 and CH_3^+.

In order to study these problems we carried out Hartree–Fock (HF), generalized valence bond (GVB), and configuration interaction (CI) calculations for a series of geometries of CH_3^+, CH_3, and CH_3^-. In all cases a good quality basis set (double zeta plus d polarization plus diffuse s and p functions) was used. Our results with regard to the above points are:

(1) CH_3 is planar with a small force constant for the out-of-plane motion.

(2) The electron affinity of CH_3^- is negative (not bound).

(3) The ν_2 vibrational frequency ofr CH_3 is calculated to be 585 cm^{-1} as compared with an experimental value [2] of 607 cm^{-1}. For CH_3^+ the calculated frequency is 1527 cm^{-1} which is to be compared with an experimental value [3] of 1360 cm^{-1} for the first Rydberg state. (The alternate experimental value [3] $\nu_2^{Ryd} = 390$ cm^{-1}, we reject on the basis of our calculations.)

2. Calculational details

2.1. Basis set and geometry

The basis set used for carbon was derived from the Dunning [4] [3s2p] contraction of Huzinaga's [5] (9s5p) set of cartesian gaussian basis functions. This set was augmented with a diffuse s function, a set of diffuse p functions and a set of d polarization func-

* Partially supported by a grant (CHE73-05132) from the National Science Foundation.

** NDEA Title IV Predoctoral Fellow. Present address: Department of Physics, University of Illinois, Urbana, Illinois 61801.

‡ Contribution No. 5463.

Table 1
Carbon basis set. Each function *nl* is expanded in terms of cartesian gaussian functions of type 1s, 2p, or 3d with coefficients as given

Function	Exponent	Coefficient
1s	4233.0	0.001220
	634.9	0.009342
	146.1	0.045452
	42.5	0.154657
	14.19	0.358866
	5.148	0.438632
	1.967	0.145918
2s	5.148	−0.168367
	0.4962	1.060091
3s	0.1533	1.0
4s	0.046	1.0
1p	18.16	0.018539
	3.986	0.115436
	1.143	0.386188
	0.3594	0.640114
2p	0.1146	1.0
3p	0.03667	1.0
1d	0.6769	1.0

tions. This basis set is summarized in table 1. The hydrogen basis is the Dunning [6] [2s] contracted set scaled to a Slater exponent of 1.2.

All geometries were taken as C_{3v} (or D_{3h} for planar) symmetry. This allows the coordinates to be completely specified by the CH bond distance and the out-of-plane angle α. (α is the angle between a CH bond and the plane perpendicular to the three-fold axis passing through the carbon.) Thus the HCH angle (θ) is given by $\cos\theta = \frac{1}{2}(3\sin^2\alpha - 1)$.

2.2. HF and GVB calculations

The HF and GVB calculations were performed to obtain preliminary information about the geometry of CH_3 and CH_3^- as well as to provide a good basis for the CI calculations. The HF wavefunctions for the (ground states of the) three systems are:

$$\Psi_{CH_3^+} = \mathcal{A}\{\phi_1^2\phi_2^2\phi_3^2\phi_4^2\alpha\beta\alpha\beta\alpha\beta\}, \quad (1a)$$

$$\Psi_{CH_3^+} = \mathcal{A}\{\phi_1^2\phi_2^2\phi_3^2\phi_4^2\phi_5\,\alpha\beta\alpha\beta\alpha\beta\alpha\}, \quad (1b)$$

$$\Psi_{CH_3^-} = \mathcal{A}\{\phi_2^2\phi_2^2\phi_3^2\phi_4^2\phi_5^2\,\alpha\beta\alpha\beta\alpha\beta\alpha\beta\}. \quad (1c)$$

From these wavefunctions the GVB wavefunction [13] can be constructed by replacing each doubly-occupied orbital with two singly-occupied orbitals,

$$\phi_i^2 \rightarrow [\phi_{ia}(1)\phi_{ib}(2) + \phi_{ib}(1)\phi_{ia}(2)], \quad (2)$$

replacing the spin function, $\alpha\beta$, with a more general spin function, and then reoptimizing all orbitals and the spin function. Generally there are no orthogonality constraints; however, in a case such as this, wherein no bonds are broken (or made) as the geometry is varied, a more restricted form can be used. The restrictions employed here are that the orbitals belonging to *different* pairs must be orthogonal and that the spin function for each pair is a singlet spin function [7]. These are referred to as the strong orthogonality (SO) and the perfect-pairing (PP) restrictions, respectively, and the wavefunction is referred to as the GVB-PP wavefunction. In solving for the GVB-PP wavefunction, each GVB pair (2) is expressed in terms of natural orbitals as

$$\phi_a\phi_b + \phi_b\phi_a = C_1\phi_1^2 + C_2\phi_2^2. \quad (3)$$

In our calculations, these restrictions are eliminated by performing appropriate configuration interaction (CI) calculations over the GVB-PP orbitals. In the GVB-PP form of the wavefunction, not all HF pairs need be replaced by GVB pairs. In particular, we did *not* correlate the C 1s pair in any of the calculations. In order to distinguish calculations with varying numbers of correlated pairs, the notation GVB(n) is used to denote a wavefunction in which n HF pairs are correlated. Thus a GVB(3) calculation for CH_3^+ is one in which the CH bond pairs are correlated and not the C 1s orbital.

The essential difference between the wavefunctions in (1) is that the singly-occupied (nonbonding) orbital of (1b) is empty in (1a) and doubly-occupied in (1c). In order to obtain consistent descriptions of these reliable values for the IP and EA it is essential to account for all correlations involving the nonbonding orbital. As a result for CH_3^- we describe the two nonbonding electrons as

$$C_1^2\phi_1^2 + C_2^2\phi_2^2 + C_3\phi_3^2 + C_4\phi_4^2, \quad (4)$$

rather than (3), thereby allowing for both the radial and angular correlations that are expected to be important for the doubly-occupied orbital. This type of wavefunction is denoted as GVB(1/4) indicating that

one pair is described in terms of four natural orbitals.

In addition to the GVB calculations, an improved virtual orbital [8] (IVO) calculation for the excited states of CH_3 was performed. The IVO calculation was based on an HF-like wavefunction using the first NO of each pair in the GVB(3-PP) wavefunction. The resulting s Rydberg orbital was used as a starting point for a GVB(3-PP) calculation of the first excited state ($^2A_1'$) of CH_3.

2.3. CI calculations

In performing the CI calculations we were seeking specifically to resolve the points given in the introduction. We wanted to look for differential correlation effects which might serve to stabilize a nonplanar structure of CH_3. We wanted to explore the stability of CH_3^-, and we wanted to obtain accurate potential curves for the ν_2 mode in CH_3 and CH_3^+. While the *valence* orbitals (that is, the NOs from the GVB space) include sufficient flexibility to describe most correlation effects, we chose to augment the valence space of GVB NOs with a set of *virtual* functions. These virtuals were obtained by starting with the diffuse s and p functions and the d functions and orthogonalizing this set to the occupied orbitals of the GVB calculation (i.e., the valence space). This procedure produces a space of 17 basis functions for CH_3 and 18 basis functions for CH_3^-. In all cases the carbon 1s orbital within this basis was fixed to be doubly-occupied.

The CI calculations performed were of two types. The first type, designed to give excitation energies, is the following:

(1) GVB-RCI – Double excitations within the valence space are allowed with the restriction that there be two electrons distributed among the NOs corresponding to each GVB pair.

(2) GVB-CI – A full CI in the valence space is performed in this case.

(3) POL-CI – All configurations of the GVB-CI are included as well as all single and double excitations from the dominant configurations with the restriction that there be at most a single excitation to the virtual space.

In performing CI calculations for ionization potentials and electron affinities, the problem is to maintain a consistent level of calculation for systems with varying numbers of electrons. A full CI on CH_3^- would include excitations one order higher than a full CI on CH_3. Thus in carrying out less than full CI calculations, one expects to include higher order excitations in CH_3^- than in CH_3 and higher order excitations in CH_3 than in CH_3^+. In particular, using an approach such as all double excitations for each system would be inconsistent. In order to treat CH_3^+, CH_3 and CH_3^- consistently with a modest computational effort, we used the following scheme, denoted IP-CI. (In each case, the excitations are from the one dominant configuration and optimum GVB orbitals are used.)

CH_3: The GVB-RCI for CH_3 plus the product of each single excitation within the valence space times each single excitation from the pi orbital to the valence or virtual space. (All excitations from the one dominant configuration.)

CH_3^+: The GVB-RCI plus all single excitations within the valence space. (This is the same as the CH_3 calculation except that the pi orbital is deleted.)

CH_3^-: the GVB-RCI plus the excitations used for CH_3 plus all double excitations from the first NO of the lone pair. (Thus we include all correlation effects used in CH_3 plus the extra correlations due to a doubly-occupied nonbonding orbital.)

3. Results

3.1. CH_3 and CH_3^+ potential curves

The results of Hartree–Fock calculations for CH_3 as a function of CH bond distance and out-of-plane angle are given in table 2. In this table we also present the optimum bond lengths and angles, obtained by fitting the calculated points with a parabola (3 points) or with cubic splines (> 3 points). This results in an optimum geometry for CH_3 of $R_{CH} = 1.070$ Å and $\theta = 2.7°$ (θ is the out-of-plane angle). This minimum is very shallow (~0.0002 eV) and as we will find below, disappears with inclusion of correlation effects. Subsequent calculations for CH_3 used only $R_{CH} = 1.075$ Å.

The GVB and CI calculations for CH_3 and CH_3^+ are presented in table 3. For the case of CH_3 we carried out GVB(3-PP), GVB-RCI, and POL-CI calculations. For CH_3^+ we used the IP-CI based on the GVB

Table 2
Hartree–Fock total energies of CH_3 as a function of bond distance and out-of-plane angle. Energies are in hartree atomic units (1 hartree = 27.2116 eV)

R_{CH} (Å)	Angle (deg)					
	0	3	5	10	19.47	Optimum angle
1.09	−39.555599	–	−39.555648	−39.555174	−39.547517	4.23°
1.075	−39.556401	−39.556409	−39.556387	−39.555756	–	3.11°
1.06	−39.556227	–	−39.556155	−39.555367	–	1.92°
Optimum R_{CH}	1.070	–	1.071	1.073	–	1.070 Å\2.72° a)

a) For each θ we used the energy at the optimum R and fitted the resulting $V(\theta)$ to obtain 2.73°.

Table 3
GVB and CI energies for CH_3, CH_3^+, CH_3^- as a function of out-of-plane angle. For CH_3 and CH_3^+ the CH bond distance is 1.075 Å, for CH_3^- it is 1.09 Å. All CI calculations are based on the GVB orbitals for CH_3 at the given geometry. Energies are in hartree atomic units

Calculation	Angle (deg)					
	0	3	5	10	19.47	30
CH_3 GVB(3-PP)	−39.599453	−39.599433	−39.599367	−39.598551	−39.598162	–
CH_3 GVB-RCI	−39.609566	−39.609473	−39.609284	−39.608021	−39.598902	–
CH_3 POL-CI	−39.634652	−39.634565	−39.634391	−39.633197	−39.624423	–
CH_3^+ IP-CI	−39.273395	−39.272219	−39.270129	−39.260299	−39.223364	–
CH_3^- GVB(1/4-PP)	−39.521362	–	–	−39.525729	−39.529839	−39.522050

orbitals for CH_3 at the same angle. The potential curves for CH_3 and CH_3^+ are shown in fig. 1. For all of the correlated wavefunctions for CH_3 (as well as for CH_3^+), the optimum angle is $\theta = 0°$. The GVB(3-PP) curve is somewhat flatter than the two CI curves for CH_3, which in turn are relatively parallel.

We find a much greater force constant for CH_3^+ than for CH_3. This is consistent with the experimental data on CH_3. Herzberg [3] gave two possible explanations of the spectrum for CH_3, both of which involve a small (580 cm^{-1}) out-of-plane vibrational frequency for CH_3 while requiring out-of-plane vibrational frequencies for the Rydberg state of either 390 cm^{-1} or 1360 cm^{-1}. Since CH_3^+ should have a frequency close to that of the Rydberg state, our results support the second assignment.

In table 4 we present the energy contributions for the dominant terms in the CI wavefunctions for CH_3, CH_3^+, and CH_3^-.

The most important correlation effect beyond GVB is the interpair type [21] which involves a simultaneous single excitation from the first to the second NO in two different bond pairs. In table 4 this is denoted as IP(a, b) where a and b are the two bond pairs. This correlation corresponds to the electrons in one pair moving in one direction (say, toward the C) while the electrons in the other pair move in the opposite direction (say, toward the H). (The spin coupling associated with this correlation is the PP or VB type.)

For CH_3 there is an important term [denoted as SC(σ, π) in table 4] in which the two orbitals of a GVB pair are coupled to triplet spin (and coupled with the π orbital to form a doublet spin state). This represents a deviation from the PP or VB spin coupling. (This term is responsible for inducing spin density into the sigma system, i.e., core polarization.) In general the energy contributions were found to vary monotonically with θ and no differential effects favoring planar geometries were found (energy contributions for $\theta = 0°$ and $\theta = 5°$ are included in table 4).

In the case of CH_3^+, there is a substantial orbital

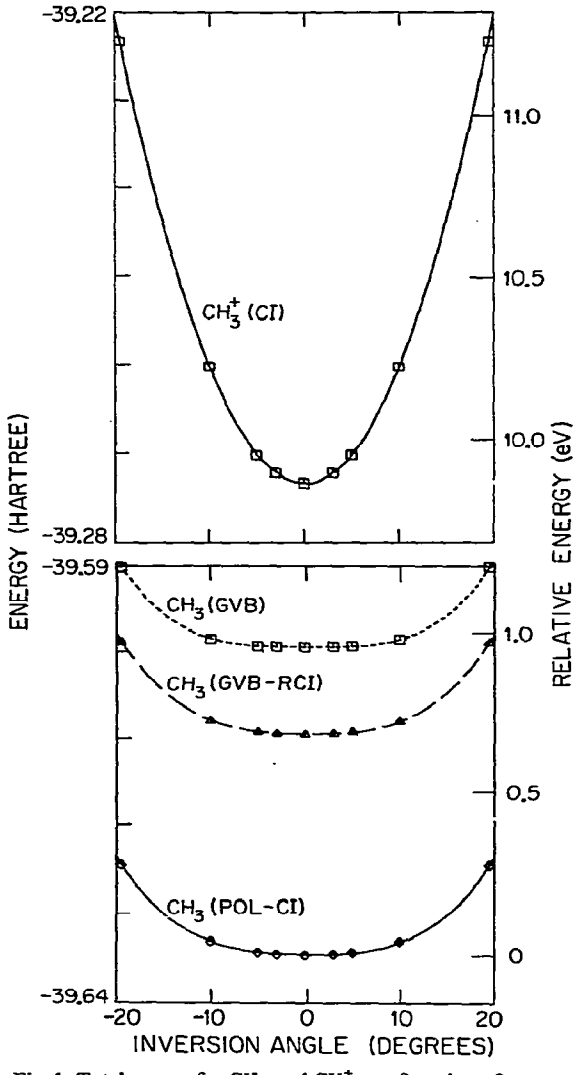

Fig. 1. Total energy for CH_3 and CH_3^+ as a function of out-of-plane angle (inversion angle).

readjustment effect (denoted as R) when the CH_3 orbitals are used for the CH_3^+ calculation. This is to be expected and disappears when the optimum CH_3^+ orbitals are used in the CI calculation (part D of table 4).

Further evidence of the monotonic nature of the bonding curve can be seen in fig. 2. Here we present orbital amplitude plots for one CH bond pair and for the singly-occupied (pi) orbital of CH_3. As the molecule is bent the pi orbital builds in a small amount of s character, thus hybridizing away from the CH bonds. Even at the tetrahedral geometry, however, this effect is not large.

3.2. CH_3^- calculations

For CH_3^- we used a CH bond length of 1.09 Å [9]. In the GVB(1/4-PP) calculations performed here, the electrons in the lone pair are allowed to correlate, reducing the effect of electron–electron repulsions. As a result, the GVB wavefunction leads to a smaller pyramidal angle, 17.4° (table 3), than does the HF wavefunction, 21.4° [10]. (Higher order correlations were carried out only for the tetrahedral bond angle of 19.47°.)

In table 5 we compare the GVB results for CH_3 and CH_3^-. With the GVB-PP wavefunctions there are only two NOs per pair. In the GVB(1/4-PP) calculation the lone pair is expanded in terms of four NOs, the first is like the HF pair, the second (σ or a_1) effects radial correlation, and the third and fourth NOs (π or e) effect angular correlation. Note that the energy lowering for the CH bond pairs is approximately the same for both systems. Inclusion of the third and fourth NOs for CH_3^- has only a small effect, 3 mhartree = 0.08 eV.

From table 6 we see that for $\theta = 19.47°$, the calculated energy of CH_3^- is 0.49 eV above the energy for CH_3 of $\theta = 0°$. The energy of CH_3 at $\theta = 19.47$ is 0.28 eV above the value for $\theta = 0°$ (POL-CI result from table 3), thus the energy of CH_3^- is 0.21 eV above that of CH_3 for the CH_3^- geometry. Hence our calculations suggest that the electron affinity of CH_3 is negative (does not bind an electron) [11]. It is well to note here that the inclusion of correlation effects leads to a decrease in the CH_3^-–CH_3 separation. For HF the separation is 1.6 eV while for GVB it is 0.84 eV and for CI it is 0.49 eV.

With additional diffuse basis functions, the electron affinity will become less negative. With sufficiently diffuse functions, one might obtain a weakly bound ($\lesssim 0.1$ eV) state for the extra electron. However, CH_3^- does not lead to a strongly bound valence-like bound state for the additional electron.

3.3. Ionization potentials

The ionization potential for CH_3 was calculated

Table 4

Energy contributions of the dominant terms in the configuration interaction wavefunctions for CH_3, CH_3^+, and CH_3^-. Included are all terms whose energy lowering[b] is greater than 1 mhartree = 10^{-3} hartree = 0.0272 eV

σ_1	σ_1^*	σ_2	σ_2^*	σ_3	σ_3^*	π	s	p_{xy}	p_z	dz^2	Type[a]	Number of equivalent cases	Total energy lowering[b] (mhartree) $\theta = 0°$	$\theta = 5°$
A. CH_3 ($^2A_2''$) using CH_3 GVB(3-PP) orbitals														
2	0	2	0	2	0	1	0	0	0	0	HF	1	–	–
0	2	2	0	2	0	1	0	0	0	0	GVB (σ_i)	3	41.29	41.19
2	0	1	1	1	1	1	0	0	0	0	IP (σ_i, σ_j)	3	4.86	4.91
2	0	2	0	1	1	1	0	0	0	0	SC (σ_i, π)	3	3.94	3.76
2	0	1	1	1	0	1	0	0	0	1		3	3.51	3.41
B. CH_3^+ ($^2A_1'$) using CH_3^+ GVB(3-PP) orbitals														
σ_1	σ_1^*	σ_2	σ_2^*	σ_3	σ_3^*	π	s	p_{xy}	p_z	dz^2			$\theta = 0°$	
2	0	2	0	2	0	0	1	0	0	0	HF	1	–	
0	2	2	0	2	0	0	1	0	0	0	GVB (σ_i)	3	38.54	
1	1	1	1	2	0	0	1	0	0	0	IP (σ_i, σ_j)	3	4.08	
2	0	2	0	1	0	0	1	0	0	1		3	4.20	
C. CH_3^+ ($^1A_1'$) using CH_3 GVB(3-PP) orbitals														
σ_1	σ_1^*	σ_2	σ_2^*	σ_3	σ_3^*	π	s	p_{xy}	p_z	dz^2			$\theta = 0°$	
2	0	2	0	2	0	0	0	0	0	0	HF	1	–	
0	2	2	0	2	0	0	0	0	0	0	GVB (σ_i)	3	35.48	
1	1	2	0	2	0	0	0	0	0	0	GVB (σ_i)	3	29.87	
2	0	2	0	1	0	0	0	1	0	0	R (σ_i)	3	5.50	
2	0	1	1	1	1	0	0	0	0	0	IP (σ_i, σ_j)	3	3.16	
2	0	2	0	1	0	0	1	0	0	0	R (σ_i)	3	2.29	
D. CH_3^+ ($^1A_1'$) using CH_3^+ GVB(3-PP) orbitals														
σ_1	σ_1^*	σ_2	σ_2^*	σ_3	σ_3^*	π	s	p_{xy}	p_z	dz^2			$\theta = 0°$	
2	0	2	0	2	0	0	0	0	0	0	HF	1	–	
0	2	2	0	2	0	0	0	0	0	0	GVB (σ_i)	3	42.32	
1	1	1	1	2	0	0	0	0	0	0	IP (σ_i, σ_j)	3	5.42	
E. CH_3^- ($^1A_1'$) using CH_3^- GVB(4-PP) orbitals														
σ_1	σ_1^*	σ_2	σ_2^*	σ_3	σ_3^*	π	π^*						$\theta = 19.47°$	
2	0	2	0	2	0	2	0				HF	1	–	
2	0	2	0	2	0	0	2				GVB (π)	3	15.80	
0	2	2	0	2	0	2	0				GVB (σ_i)	3	37.40	
2	0	2	0	1	1	1	1				IP (σ_i, π)	3	10.59	
1	1	1	1	2	0	2	0				IP (σ_i, σ_j)	3	4.60	

[a] IP indicates an interpair correlation term. R indicates an orbital readjustment term. SC indicates a spin-coupling term.

[b] The energy contribution (in mh) is defined as the change in energy when the configuration is deleted from the wavefunction while keeping all other CI coefficients fixed.

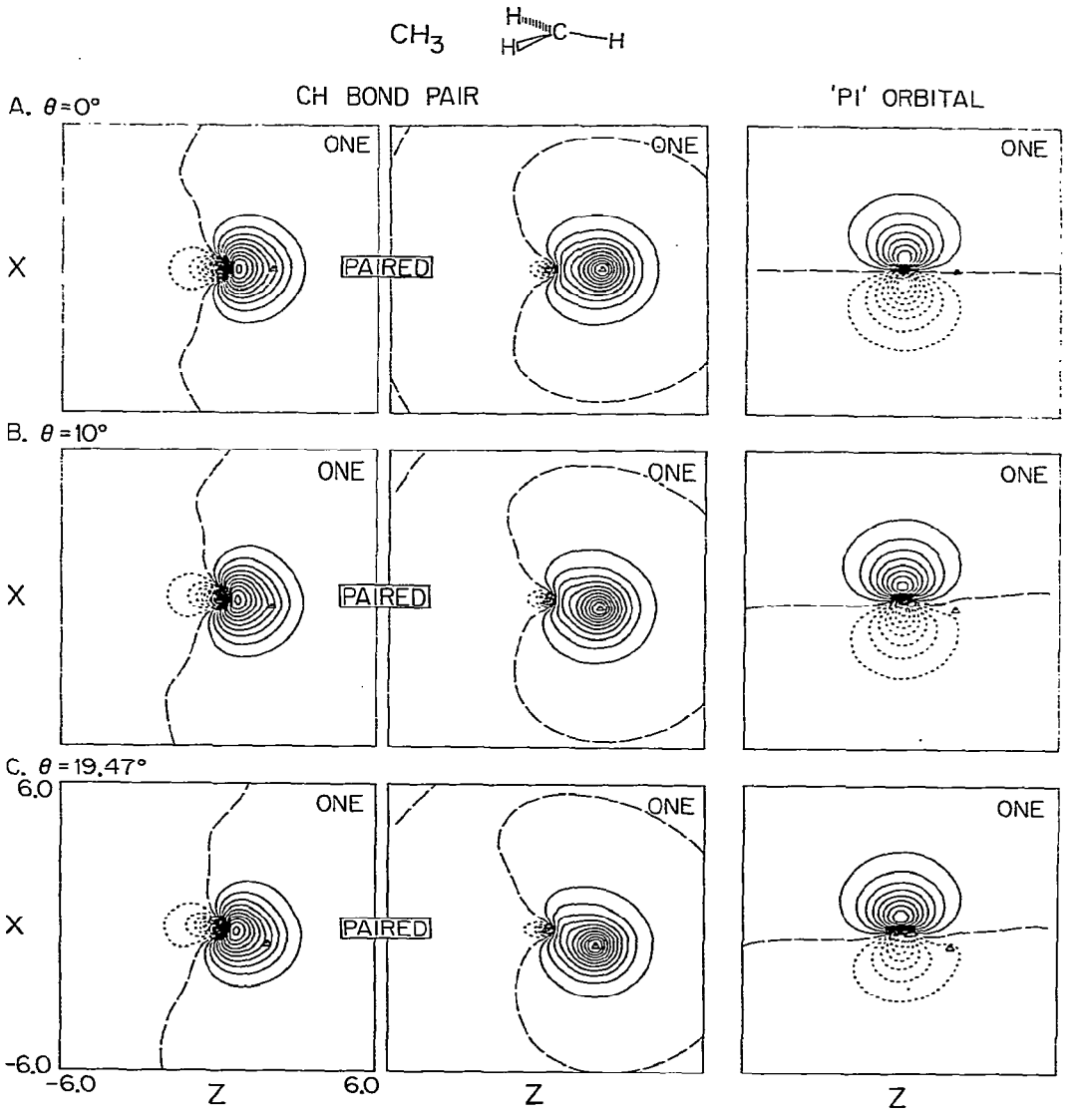

Fig. 2. Orbital amplitude plots for one CH bond pair and the nonbonding orbital of CH_3 from the GVB(3-PP) wavefunction for various out-of-plane angles. The contour interval is 0.05 au, positive contours are solid, negative contours are short dashes, zero amplitude is represented by long dashes.

by performing a GVB(3-PP) calculation on CH_3^+ and then using those orbitals as the basis for an IP-CI. The results of this calculation are given in table 6. The GVB calculations lead to an ionization potential of 8.86 eV, in very good agreement with the HF result of Driessler et al. [15]. The IP-CI ionization potential is 9.52 eV while the experimental result is 9.83 eV [12]. The IP-CI based on the CH_3 ground state orbitals (used for the bending curve) gives an ionization potential of 9.71 eV, the better agreement being due to a poorer description of CH_3^+. From table 4 we see that in the case of both CH_3 and CH_3^+

Table 5
Comparison of energy contributions for GVB wavefunctions of CH_3 and CH_3^-

Calculation	Angle (deg)	R_{CH} (Å)	Total energy (hartree)	Energy lowering[a] (mhartree)[b]	
CH_3 GVB(3-PP)	0	1.075	−39.59945	14.44	CH bond (3)
CH_3 GVB(3-PP)	19.47	1.09	−39.59108	14.65	CH bond (3)
CH_3^- GVB(4-PP)	19.47	1.09	−39.56862	14.40	CH bond (3)
				22.67	lone pair (1)
CH_3^- (GVB(1/4-PP)	19.47	1.09	−39.52984	25.78	lone pair (1)

[a] Energy lowering per bond or electron pair. [b] 1 mhartree = 10^{-3} hartree ≈ 0.0272 eV.

Table 6
Comparison of calculated energies for CH_3, CH_3^+ and CH_3^-. Energies are in hartree atomic units unless otherwise noted

Calculation	$CH_3(^2A_2'')$ $\theta = 0°$	$CH_3^+(^2A_1')$ $\theta = 0°$	$CH_3^-(^1A_1)$ $\theta \approx 19.47°$	$CH_3^+(^1A_1)$ $\theta = 0°$
GVB-PP	−39.59945	−39.38096	−39.56862	−39.27400
GVB-RCI	−39.60957	–	−39.58869	–
IP-CI	−39.63018	–	−39.61222	−39.28040[d]
POL-CI	−39.63465	−39.41142	–	–
Relative energy[a] (hartree)	0.0	0.2232	0.01796	0.3498[d]
(eV)	0.0	6.07	0.49	9.52
Experiment (eV)	0.0	5.73[b]	–	9.83[c]

[a] Based on IP-CI except for CH_3 ($^2A_1'$) which is based on POL-CI. [b] Ref. [3]. [c] Ref. [12]. [d] Using CH_3 orbitals we obtain $E = -39.27340$ hartree and an IP of 9.71 eV.

the dominant terms in the CI wavefunction come from the GVB-RCI configuration. It should be noted that there is not sufficient flexibility in the CI basis to adequately describe all correlations between the bond pairs and the pi orbital. Thus we expect to find that the CH_3 energy is too high relative to the CH_3^+ energy.

3.4. Excitation energies

For the fixed planar geometry, there are no low-lying valence excited states for CH_3; the first excitation is from the pi orbital to a 3s-like Rydberg orbital. Although our basis does not include functions quite diffuse enough for the Rydberg states (an outer s exponent of 0.021 being more appropriate [4]), we carried out calculations for these states in order to examine their overall character. As a first approximation to the excited states, we solved for the excited states using the IVO method [8]. These energies are given in table 7, and the resulting orbitals are displayed in fig. 3, where their Rydberg nature is easily seen. Subsequently a GVB(3-PP) calculation for the $^2A_1'$ states was performed and the resulting

Table 7
IVO results for the first Rydberg state of CH_3

State	Singly-occupied orbital	(type)	Orbital energy (hartree)	Excitation energy (eV)
$^2A_2''$	$2p_\pi$	(val)	−0.372423	0.0
$^2A_1'$	3s	(ryd)	−0.131569	6.55[a]
$^2E'$	$3p_\sigma$	(ryd)	−0.087838	7.74
$^2A_2''$	$3p_\pi$	(ryd)	−0.073088	8.15

[a] GVB-CI leads to $\Delta E = 6.07$ eV while experiment leads to 5.73 eZ, see table 6.

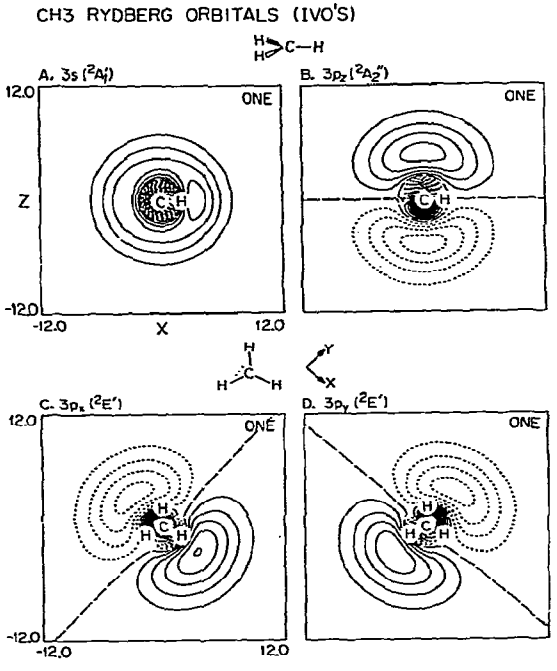

Fig. 3. Orbital amplitude plots for the Rydberg orbitals for CH_3. The contour interval is 0.01 au.

orbitals were used for a POL-CI calculation. These results (see table 6) lead to a calculated excitation energy of 6.07 eV as compared with an experimental value of 5.73 eV [3]. As mentioned, above additional more diffuse basis functions should be included for a good description of the Rydberg states.

4. Vibrational frequencies

In calculating vibrational frequencies, there are two ways to proceed once the potential curves are available. One is to use a (harmonic) valence force field approximation based on the curvatures of the potential curves (see the Appendix), while the other is to solve numerically for the vibrational wavefunctions and eigenvalues of the calculated (nonharmonic) potential curves [14]. For the purpose of comparison we have done both. The valence force field results are given in table 8 while the results of the numerical solution for the vibrational energy levels are given in table 9. Only the first two levels are reported in this latter case since the vibrational wavefunctions for the higher levels have significant amplitude outside the region ($|\theta| < 20°$) for which the potential was calculated. The potential curves used for the numerical solutions were POL-CI for CH_3 and IP-CI for CH_3^+.

For CH_3 we find that the harmonic approximation gives terrible results, due to the anharmonic shape of the potential curve. The GVB(3-PP) curve gives a vibrational frequency of $\bar{\nu}_2^H = 113$ cm^{-1} while the GVB-RCI and POL-CI curves give $\bar{\nu}_2^H = 396$ cm^{-1} and $\bar{\nu}_2^H = 390$ cm^{-1}, respectively. Using the POL-CI curve the numerical integration results in a vibrational frequency of $\bar{\nu}_2 = 585$ cm^{-1} for CH_3 and $\nu_2 = 430$ cm^{-1} for CD_3. This compares favorably with the gas phase infrared results [2] of $\bar{\nu}_2 = 607$ cm^{-1} for CH_3 and $\bar{\nu}_2 = 461$ cm^{-1} CD_3.

In the case of CH_3^+ we find that the harmonic approximation is adequate. The calculated frequency in that case is 1564 cm^{-1} while the numerical integration result is 1527 cm^{-1}. For CD_3^+ the numerical integration yielded a value of 1192 cm^{-1}. Experimentally, the vibrational frequency for CH_3^+ has not been measured directly. Herzberg [3] has proposed two possible assignments of the spectrum for CH_3 leading to two possible vibrational frequencies for the first s-Rydberg state. In both assignments the out-of-plane

Table 8
Force constants and vibrational frequencies for CH_3 and CH_3^+ using the harmonic valence force field approximation (see Appendix)

Calculation	Curvature (hartree/deg^2)	k_Δ/l^2 (mdyn/A)	$\bar{\nu}$ (cm^{-1})
CH_3			
GVB(3-PP)	1.4696×10^{-6}	6.067×10^{-3}	113
GVB-RCI	1.8053×10^{-5}	7.453×10^{-2}	396
POL-CI	1.7471×10^{-5}	7.213×10^{-2}	390
CH_3^+			
IP-CI	2.8127×10^{-4}	1.161	1564

Table 9
Vibrational energies for CH_3, CH_3^+, CD_3 and CD_3^+. (From numerical solution of the vibrational wavefunctions using the CI potential curves[d])

Level	Energy (hartree)	$\bar{\nu}$ (cm^{-1})	Experiment (cm^{-1})
CH_3			
E_0	−39.634651		
$\nu = 0$	−39.633494	(253.9)[c]	
$\nu = 1$	−39.630829	584.9	607[b]
CD_3			
E_0	−39.634651		
$\nu = 0$	−39.633790	(188.9)[c]	
$\nu = 1$	−39.631831	429.9	460[b]
CH_3^+			
E_0	−39.273590		
$\nu = 0$	−39.270188	(746.6)[c]	
$\nu = 1$	−39.263227	1527.8	(~1370)[a]
CD_3^+			
E_0	−39.273590		
$\nu = 0$	−39.270972	(574.6)[c]	
$\nu = 1$	−39.265543	1191.5	(~1030)[a]

[a] Based on the lowest Rydberg excited state rather than the positive ion state, ref. [3]. [b] Ref. [2]. [c] This is the calculated zero-point energy. [d] The calculated points were interpolated using cubic splines.

vibrational frequency was assumed to be $\bar{\nu}_2^{CH_3} = 580$ cm^{-1}. The first assignment gives a vibrational frequency of $\bar{\nu}_2^{Ryd} = 390$ cm^{-1} for the out-of-plane bend in the s-Rydberg state while the second assignment gives a vibrational frequency of $\bar{\nu}_2^{Ryd} = 1360$ cm^{-1}. The influence of the single electron in the Rydberg orbital on the vibrational frequency should be sufficiently small that the bending frequency found by Herzberg is only slightly different from the value for CH_3^+. This being the case, it is quite clear from the potential curves that the second assignment of Herzberg is the proper one. Thus our values of $\bar{\nu}_2 = 1527$ cm^{-1} and $\bar{\nu}_2 = 1192$ cm^{-1} for CH_3^+ and CD_3^+, respectively should be compared with the experimental values of $\bar{\nu}_2 = 1360$ cm^{-1} and $\bar{\nu}_2 = 1030$ cm^{-1} for the Rydberg state. A portion of this discrepancy could be a real difference in ν_2 for the Rydberg state as compared with the ion state.

5. Discussion

Recently, Koenig et al. [1] observed a photoelectron spectrum of CH_3 in which there was a vibrational progression corresponding to a frequency of 720 cm^{-1}. They interpreted this progression as being due to the excitation of the out-of-plane bend in CH_3^+, which was excited because the CH_3 ground state "is not strictly planar". In view of the discussion in the previous section, this interpolation is incorrect on the basis of our calculations and of *either* of Herzberg's assignments. Recently Dyke et al. [26], Koenig et al. [27], and Houle [23] suggested that the 720 cm^{-1} bands arise from $\upsilon = 1$ vibrational levels of CH_3 (leading, for example, to 1–1 bands separated by $\nu_2^{CH_3^+} - \nu_2^{CH_3} \approx 1360 - 607 = 753$ cm^{-1} from 0–0); this would appear to explain the observed structure.]

A simple qualitative analysis for understanding the geometries of CH_3^+, CH_3, and CH_3^- is to start with the appropriate ion of CH_2 and to examine where the added H should go. The ground state of CH_2 is the $^3B_1(\sigma\pi)$ state [24]

(5)

with one electron each on the σ and π nonbonding orbitals. The σ orbital is lower than the π orbital (for HCH bond angles less than 180°) so that CH_2^+ is the $^2B_1(\sigma)$ state

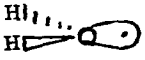

(6)

while CH_2^- is the $^2B_1(\sigma^2\pi)$ state

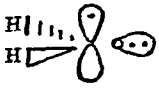

(7)

Since the radical orbital of CH_2^+ (6) is in the HCH plane, an additional H atom should strongly favor the planar geometry of CH_3^+. Since the radical orbital of CH_2^- (7) is perpendicular to the HCH plane, an additional H atom should strongly favor the pyramidal geometry of CH_3^-. [As the new bond is formed, there are repulsive interactions (resulting from the Pauli principle) between the new bond pair and the old

ones, leading to some opening of the bond angle.] Since the neutral form of CH_2 (5) has two radical orbitals, we can form either planar or pyramidal geometries of CH_3 without promoting the electronic state of the CH_2; hence the potential surface is expected to be flat. However, binding the new H to the σ orbital leads to smaller overlaps with the other two CH bonds (and hence smaller repulsive interactions arising from the Pauli principle) than does bonding the H to the π orbital. Consequently, the planar form of CH_3 is favored [24], but only slightly.

In contrast, the ground state of CF_2 is the $^1A_1$ state leading to nonbonding orbitals of the form [24]

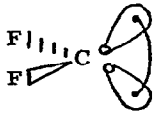

(8)

As a result, adding the third F leads to a nonplanar geometry for CF_3 [24].

6. Comparison with previous calculations

There have been a number of calculations on the three species considered herein, with general agreement on the geometries [10,15,16,17,22]. CH_3^+ and CH_3 are generally found to be planar with CH_3^+ having a considerably larger force constant. CH_3^- is always found to be nearly tetrahedral; however, CH_3^- is generally found to be unstable with respect to CH_3 and an electron.

There seems to be some misunderstanding with regard to the calculation of vibrational frequencies for the inversion or umbrella mode. Kari and Csizmadia [10] quote a frequency of $\nu_2 = 746$ cm^{-1} for CH_3^+ as corresponding to a force constant of 1.63 mdyn/Å. Their potential curve is virtually parallel to ours and we interpret their data as giving a force constant of 1.166 mdyn/Å corresponding to a vibrational frequency of $\nu_2 = 1568$ cm^{-1} (the experimental value for the Rydberg state is 1360). In addition, we find that the inversion force constants for CH_3 reported by Millie and Berthier [16] should be 0.0075 mdyn/Å (instead of 0.014 mdyn/Å), leading to a vibrational frequency of 126 cm^{-1}. These discrepancies have led us to include an Appendix on the precise formulae we used in determining force constants.

For CH_3^+ the out-of-plane force constants in the literature are in the range 0.96–1.16 mdyn/Å, whereas our value is 1.16 mdyn/Å. For CH_3 there is a wide variation in the out-of-plane force constant, depending on the basis set and type of calculation. Indeed, we find that the harmonic approximation for CH_3 is particularly unreliable, leading to a ν_2 significantly smaller (by 33%) than the value from the numerical solution of the vibrational wavefunctions.

We do find some discrepancy between our calculations and those of Driessler et al. [15], namely, (i) they find CH_3^- to be stable relative to CH_3 and an electron by 0.11 eV, while we find it to be unstable by 0.49 eV [25] and (ii) their potential curve for CH_3 leads to a force constant about twice our value.

Driessler et al. carried out HF calculations for CH_3, CH_3^+, and CH_3^-, and then calculated the correlation energies using a Bethe–Goldstone type method (IEPA), obtaining correlation energies of 0.148, 0.184, 0.239 hartree, respectively. A potential difficulty here is that the IEPA method does not provide a bound on the total energy, and hence comparisons of systems with different configurations or different numbers of electrons may lead to inconsistent results. For example, Ahlrichs et al. [19] found that using a "better" method the correlation energy for CH_3^- becomes 0.199 h. Such a decrease of 0.05 h = 1.36 eV in the relative correlation energy of CH_3^- and CH_3 is more than sufficient to bring the Driessler et al. results into agreement with ours.

For the potential curve of CH_3, we find a ν_2 of 585 cm^{-1}, in good agreement with the experimental value of 607 cm^{-1}. Driessler et al, in their IEPA calculations, find a force constant over twice as large as ours and hence we expect that their potential curve would lead to an inversion frequency of 850 cm^{-1} (if calculated numerically), considerably above the experimental value.

7. Conclusion

We find that CH_3 is planar although its potential curve for the out-of-plane is very flat, leading to a large zero-point motion. The potential curves for CH_3 and CH_3^+ are *quite* different and any experimental information relating to these two species should be interpreted in that light. We find that CH_3^- is unstable

with respect to CH_3 plus an electron (that is, the electron affinity is negative).

One of us (GTS) would like to thank Frances Houle for discussions and encouragement and Professor S.I. Chan for helpful discussions.

Note added in proof: Marynick and Dixon [28] recently reported theoretical results in agreements with ours.

Appendix: Calculation of vibrational frequencies

In the harmonic valence force field approximation, the potential is of the form (following Herzberg [20], p. 178)

$$V = \tfrac{1}{2}k_\Delta(\Delta_{12}^2 + \Delta_{13}^2 + \Delta_{14}^2),$$

where Δ is the deviation from planar. For distortions of C_{3v} symmetry the energy is

$$E(\theta) = E_0 + \tfrac{1}{2}(d^2E/d\theta^2)\theta^2,$$

and

$$k_\Delta = \tfrac{1}{3}d^2E/d\theta^2$$

(we obtain the curvature $d^2E/d\theta^2$ from a cubic spline fit to the calculated points). In cgs units the vibrational wavenumber is given by (ref. [20], p. 178)

$$\bar{\nu}(cm^{-1}) = 2256.48\sqrt{\bar{k}}(mdyn/Å)/\mu(AMU),$$

where $\bar{k} = k_\Delta/l^2$,

$$\mu(AMU) = M_H M_C/(M_C + 3M_H),$$

using atomic mass units ($\mu = 0.805253$ for CH_3 and 1.34001 for CD_3), and

$$\bar{k}(mdyn/Å) = 4128.33(d^2E/d\theta^2)(hartree/deg^2).$$

References

[1] T. Koenig, T. Balle and W. Snell, J. Am. Chem. Soc. 97 (1975) 662.
[2] L.Y. Tan, A.M. Winer and G.C. Pimentel, J. Chem. Phys. 57 (1972) 4028.
[3] G. Herzberg, Proc. Roy. Soc. A262 (1961) 291.
[4] T.H. Dunning, Jr. and P.J. Hay, in: Modern Theoretical Chemistry: Electronic Structure, ed. H.F. Schaefer III (Plenum, New York, 1976), Vol. II, to be published. This is not the [3s2p] basis of ref. [6].
[5] S. Huzinaga, J. Chem. Phys. 42 (1965) 1293.
[6] T.H. Dunning, J. Chem. Phys. 53 (1970) 2823.
[7] W.J. Hunt, P.J. Hay and W.A. Goddard III, J. Chem. Phys. 57 (1972) 738.
[8] W.J. Hunt and W.A. Goddard III, Chem. Phys. Lett. 3 (1969) 414.
[9] Standard bond length from J.A. Pople and M. Gordon, J. Am. Chem. Soc. 89 (196) 4253.
[10] R.E. Kari and I.G. Csizmadia, J. Chem. Phys. 50 (1969) 1443.
[11] We have not optimized the geometry of CH_3^- and thus should overestimate the CH_3^-–CH_3 energy separation. However, such effects should be smaller than the calculated energy separation.
[12] L. Golob, N. Jonathan, A. Moras, M. Okuda and K. Ross, J. Electron. Spectrosc. Relat. Phenomena 1 (1973) 506.
[13] R.C. Ladner and W.A. Goddard III, J. Chem. Phys. 51 (1969) 1073;
W.A. Goddard III and R.C. Ladner, J. Am. Chem. Soc. 93 (1971) 6750.
[14] The computer program for solving the one-dimensional vibrational wavefunctions was written by R.C. Ladner for diatomic systems based on Cooley's method [Math. Comp. 15 (1961) 363] and modified for variable effective masses by D.B. Olafson.
[15] F. Driessler, R. Ahlrichs, B. Staemmler and W. Kutzel Kutzelnigg, Theor. Chim. Acta 30 (1973) 315.
[16] P. Millie and G. Berthier, Int. J. Quantum Chem. 2S (1968) 67.
[17] S.Y. Chang, E.R. Davidson and G. Vincow, J. Chem. Phys. 52 (1970) 5596.
[18] H.F. Schaefer III, The Electronic Structure of Atoms and Molecules (Addison–Wesley, Reading, Mass., 1972) p. 129.
[19] R. Ahlrichs, H. Lischka, V. Staemmler and W. Kutzelnigg, J. Chem. Phys. 62 (1975) 1225, 1245.
[20] G. Herzberg, Molecular Spectra and Molecular Structure. II. Infrared and Raman Spectra of Polyatomic Molecules (Van Nostrand, New York, 1945).
[21] L.B. Harding and W.A. Goddard III, J. Am. Chem. Soc. 97 (1975) 6293.
[22] K. Morokuma, L. Pedersen and M. Karplus, J. Chem. 48 (1968) 4801.
[23] F. Houle, private communication.
[24] W.A. Goddard III, T.H. Dunning, Jr., W.J. Hunt and P.J. Hay, Accts. Chem. Res. 6 (1973) 368.
[25] Of course, inclusion of sufficiently diffuse functions would allow this energy difference to go to zero. However, our basis is appropriate to bound negative ions and hence the calculated energy difference of 0.49 eV is a good indication of how much stabilization is required to make the electron of CH_3^- bound (for example, by substitution of the H with appropriate ligands).
[26] J. Dyke, N. Jonathan, E. Lee and A. Morris, J. Chem. Soc., Faraday Trans. II 72 (1976) 1385.
[27] T. Koenig, T. Balle and J.C. Chang, Spectrosc. Lett. (in press).
[28] D.S. Marynick and D.A. Dixon, Proc. Natl. Acad. Sci. USA 74 (1977) 410.